Electronic Supplementary Information (ESI) for

Solvent Effects on Surface-grafted and Solution-born poly[*N*-(2-hydroxypropyl) methacrylamide] during Surface-initiated RAFT Polymerization

Yu-Min Wang,[*a] Anna Kálosi,[b,c] Yuriy Halahovets,[c] Hynek Beneš,[a] Andres de los Santos Pereira[a] and Ognen Pop-Georgievski[*a]

[a] Institute of Macromolecular Chemistry, Czech Academy of Sciences, Heyrovského nám. 2, 16200 Prague, Czech Republic

[b] Centre for Advanced Materials Application, Slovak Academy of Sciences, Dúbravská cesta 9, 84511 Bratislava, Slovakia

[c] Department of Multilayers and Nanostructures, Institute of Physics, Slovak Academy of Sciences, Dúbravská cesta 9, 84511 Bratislava, Slovakia

Corresponding Authors:

*e-mail: wang@imc.cas.cz; georgievski@imc.cas.cz

Calculation of apparent propagation rate

When the polymerization followed the near-linear pseudo-first-order kinetic, the termination and transfer reaction were suppressed. Assuming a fast initiation step, the rate of polymerization is given by:

$$R_{\mathrm{p}} = -\frac{d[M]}{dt} = k_{\mathrm{p}}[P^*][M] \qquad \text{(Equation S1)},$$

where [M] is the monomer concentration, k_{p} is the propagation rate constant, and [P^*] is the concentration of active chain ends. In the absence or suppression of termination, [P^*] is constant, and the product k_{p} [P^*] can be regarded as an apparent propagation rate constant ($k_{p,\ \mathrm{app}}$). Introducing monomer conversion, integration of equation S1 leads to:

$$ln\frac{[M]_0}{[M]_{\mathrm{t}}} = k_{\mathrm{p}}[P^*]t = k_{\mathrm{p},\ \mathrm{app}}t \qquad \text{(Equation S2)}.$$

Size exclusion chromatography (SEC) traces for solution-born p(HPMA)

All curves from the SEC/refractive index detector are normalized to the same ordinate scale at each representative SEC graph.

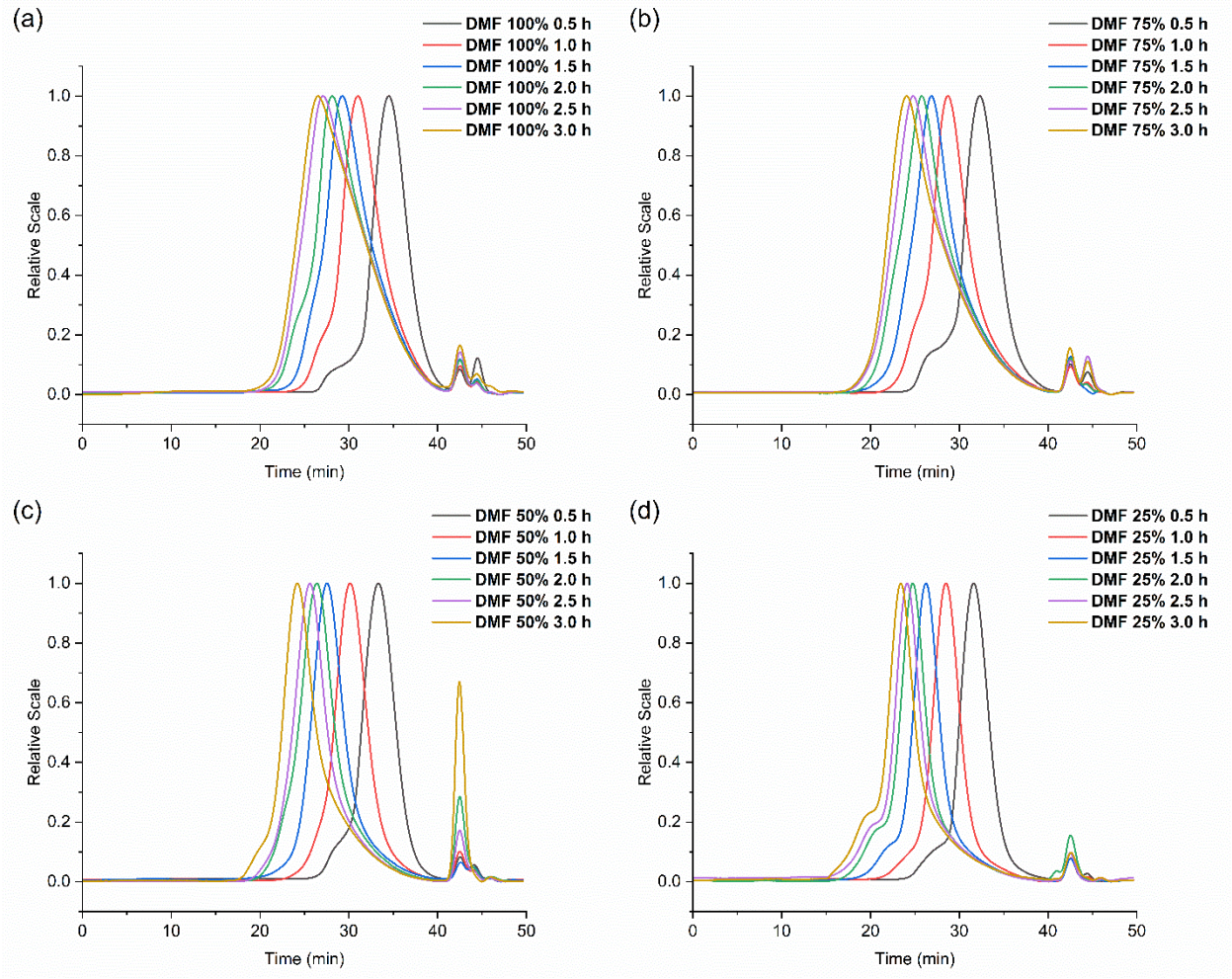

Figure S1. Evolution of SEC traces (differential refractive index detector) of solution-born p(HPMA) with different reaction times during SI-RAFT polymerization at conditions (a) DMF 100%, (b) DMF 75%, (c) DMF 50%, and (d) DMF 25%.

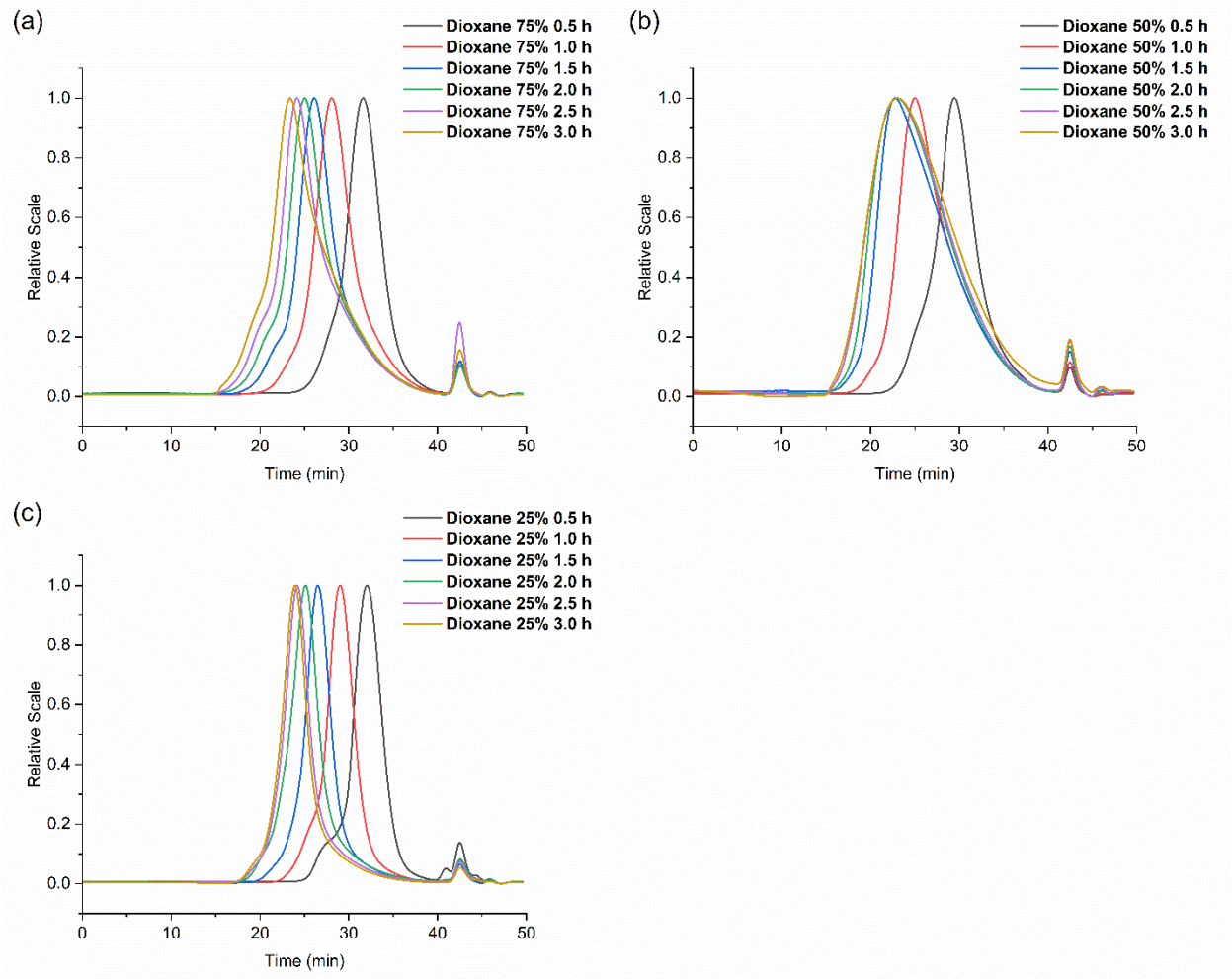

Figure S2. Evolution of SEC traces (differential refractive index detector) of solution-born p(HPMA) with different reaction times during SI-RAFT polymerization at conditions (a) 1,4-Dioxane 75%, (b) 1,4-Dioxane 50%, and (c) 1,4-Dioxane 25%.

Table S1. Macromolecular parameters of solution-born p(HPMA) in DMF condition.

Entry	Solvent conditions	Macromolecular parameters	Time (h)					
			0.5	1.0	1.5	2.0	2.5	3.0
1	DMF 100%	Conversion (%)	3.2 ± 0.3	6.9 ± 2.3	12.2 ±1.6	15.0 ± 1.9	17.3 ± 2.5	20.5 ± 3.7
		Number-average $M_{n,\,sol}$ ($kg{\cdot}mol^{-1}$)	14.5 ± 2.9	25.6 ± 3.9	34.0 ± 2.6	37.5 ± 3.4	41.9 ± 5.0	44.9 ± 3.3
		Dispersity, $Đ$	1.33 ± 0.05	1.31 ± 0.02	1.39 ± 0.03	1.48 ± 0.07	1.47 ± 0.02	1.51 ± 0.07
2	DMF 75%	Conversion (%)	4.6 ± 1.0	11.4 ± 2.5	16.7 ± 4.6	20.8 ± 4.0	26.8 ± 3.3	32.6 ± 5.0
		Number-average $M_{n,\,sol}$ ($kg{\cdot}mol^{-1}$)	26.3 ± 2.3	44.4 ± 4.8	58.3 ± 4.7	66.0 ± 3.4	72.5 ± 4.0	79.3 ± 2.2
		Dispersity, $Đ$	1.28 ± 0.02	1.26 ± 0.01	1.29 ± 0.03	1.40 ± 0.06	1.43 ± 0.08	1.39 ± 0.09
3	DMF 50%	Conversion (%)	4.6 ± 2.4	12.5 ± 4.4	17.7 ± 2.9	21.8 ± 5.2	28.5 ± 8.1	36.8 ± 10.5
		Number-average $M_{n,\,sol}$ ($kg{\cdot}mol^{-1}$)	29.9 ± 6.1	51.6 ± 11.6	67.5 ± 6.7	83.8 ± 7.6	93.0 ± 8.8	101.2 ± 9.0
		Dispersity, $Đ$	1.22 ± 0.02	1.25 ± 0.10	1.26 ± 0.05	1.30 ± 0.11	1.32 ± 0.09	1.37 ± 0.13
4	DMF 25%	Conversion (%)	4.4 ± 2.2	12.7 ± 2.1	20.3 ± 3.3	23.0 ± 9.7	39.9 ± 1.5	42.2 ± 2.8
		Number-average $M_{n,\,sol}$ ($kg{\cdot}mol^{-1}$)	38.5 ± 3.2	64.4 ± 5.1	91.1 ± 7.7	108.5 ± 5.5	123.1 ± 7.5	124.8 ± 7.7
		Dispersity, $Đ$	1.19 ± 0.01	1.18 ± 0.05	1.23 ± 0.06	1.30 ± 0.02	1.30 ± 0.03	1.40 ± 0.07

Table S2. Macromolecular parameters of solution-born p(HPMA) in 1,4-Dioxane condition.

Entry	Solvent conditions	Macromolecular parameters	Time (h)					
			0.5	1.0	1.5	2.0	2.5	3.0
5	1,4-Dioxane 75%	Conversion (%)	9.4 ± 5.5	14.8 ± 5.2	25.0 ± 2.8	27.9 ± 1.8	32.2 ± 1.5	41.3 ± 3.5
		Number-average $M_{n,\,sol}$ ($kg \cdot mol^{-1}$)	37.2 ± 5.2	58.7 ± 4.2	73.3 ± 8.6	89.0 ± 15.2	95.5 ± 12.2	95.3 ± 6.5
		Dispersity, $Đ$	1.26 ± 0.05	1.29 ± 0.04	1.34 ± 0.11	1.34 ± 0.13	1.41 ± 0.11	1.48 ± 0.08
6	1,4-Dioxane 50%	Conversion (%)	17.1 ± 4.0	24.0 ± 5.6	34.0 ± 2.3	44.7 ± 3.0	51.3 ± 6.4	57.7 ± 8.5
		Number-average $M_{n,\,sol}$ ($kg \cdot mol^{-1}$)	51.5 ± 3.5	69.0 ± 2.2	90.5 ± 11.8	89.3 ± 18.1	92.2 ± 11.1	94.0 ± 1.6
		Dispersity, $Đ$	1.29 ± 0.06	1.42 ± 0.10	1.42 ± 0.19	1.60 ± 0.26	1.63 ± 0.14	1.64 ± 0.20
7	1,4-Dioxane 25%	Conversion (%)	8.5 ± 1.0	18.1 ± 4.9	26.4 ± 3.5	34.0 ± 5.5	39.8 ± 6.9	49.9 ± 9.0
		Number-average $M_{n,\,sol}$ ($kg \cdot mol^{-1}$)	44.0 ± 9.3	75.5 ± 14.8	102.2 ± 16.0	118.0 ± 15.9	139.2 ± 22.2	157.7 ± 25.8
		Dispersity, $Đ$	1.17 ± 0.01	1.19 ± 0.06	1.26 ± 0.13	1.33 ± 0.16	1.36 ± 0.17	1.42 ± 0.29

Analysis of SMFS data using the worm-like chain (WLC) model for surface-grafted p(HPMA)

Each force-distance curve showing rupture events was fitted using the WLC model:

$$f(x) = \frac{k_\mathrm{b}T}{l_\mathrm{p}}\left[\frac{1}{4\left(1-\frac{x}{l_\mathrm{c}}\right)^2} - \frac{1}{4} + \frac{x}{l_\mathrm{c}}\right] \qquad \text{(Equation S3)}$$

where x is the distance of the AFM tip from the surface, f is the pull-off force, k_b is Boltzmann constant, T is the absolute temperature. The persistence length l_p and the contour length l_c are the two unknown parameters which are directly obtained from the fit of the individually measured force-distance curves. The determined values of the persistence length l_p are in the range of 0.2–0.3 nm. The full length of the polymer chain contributes to l_c, as the polymer chains are bound through their chain-ends when stretched between the surface and the AFM tip.[1-4] The determined value of the contour length l_c can thus be reliably utilized for the calculation of the molar mass of a surface-grafted polymer chain M_sur as:

$$M_\mathrm{sur} = M_\mathrm{HPMA}\frac{l_\mathrm{c}}{l_\mathrm{HPMA}} \qquad \text{(Equation S4)}$$

with the molar mass of HPMA monomer to be $M_{HPMA} = 143.2$ g·mol^{-1} and the length of the monomer (C–C–C bonds along the main chain) to be $l_{HPMA} = 2.73$ Å.[3, 5] Accordingly, we obtained the molar mass M_sur distributions of surface-grafted polymers polymerized in different solvent systems at various polymerization times (Figure S5-8). Table S3 reports the number-averaged contour lengths ($l_{\mathrm{n,\ c}} = \frac{1}{n}\sum l_\mathrm{c}$) and molar masses of surface-grafted polymers ($M_{\mathrm{n,\ sur}} = \frac{1}{n}\sum M_\mathrm{sur}$) obtained from the analysis of the SMFS data.

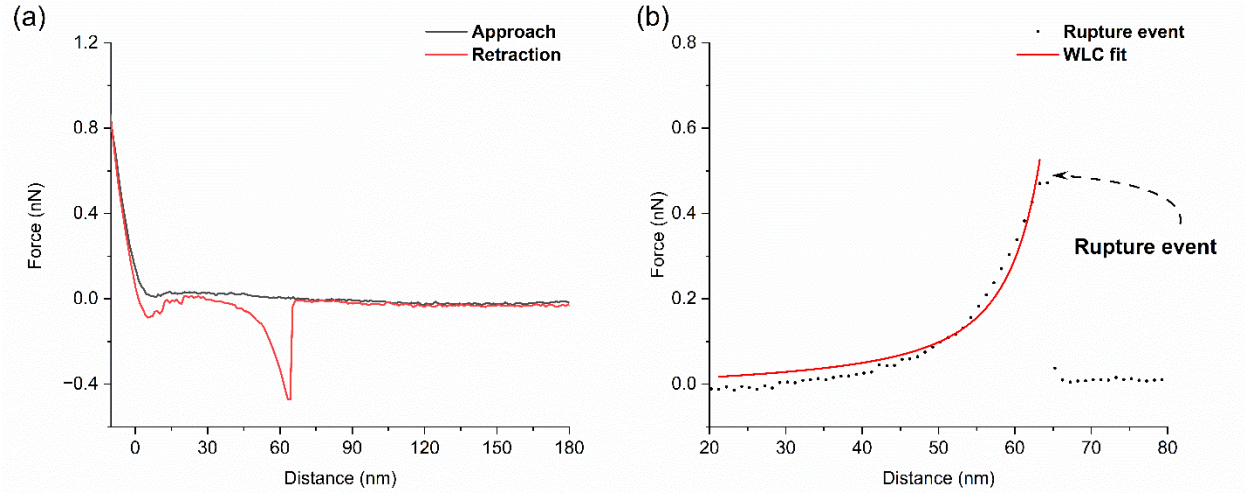

Figure S3. (a) Representative force–distance curve of selected clear unfolding and rupture event during approach (black line) and retraction (red line) of the AFM tip. (b) Characteristic pull-off force curve (black square symbols) fitted according to the WLC model (red line).

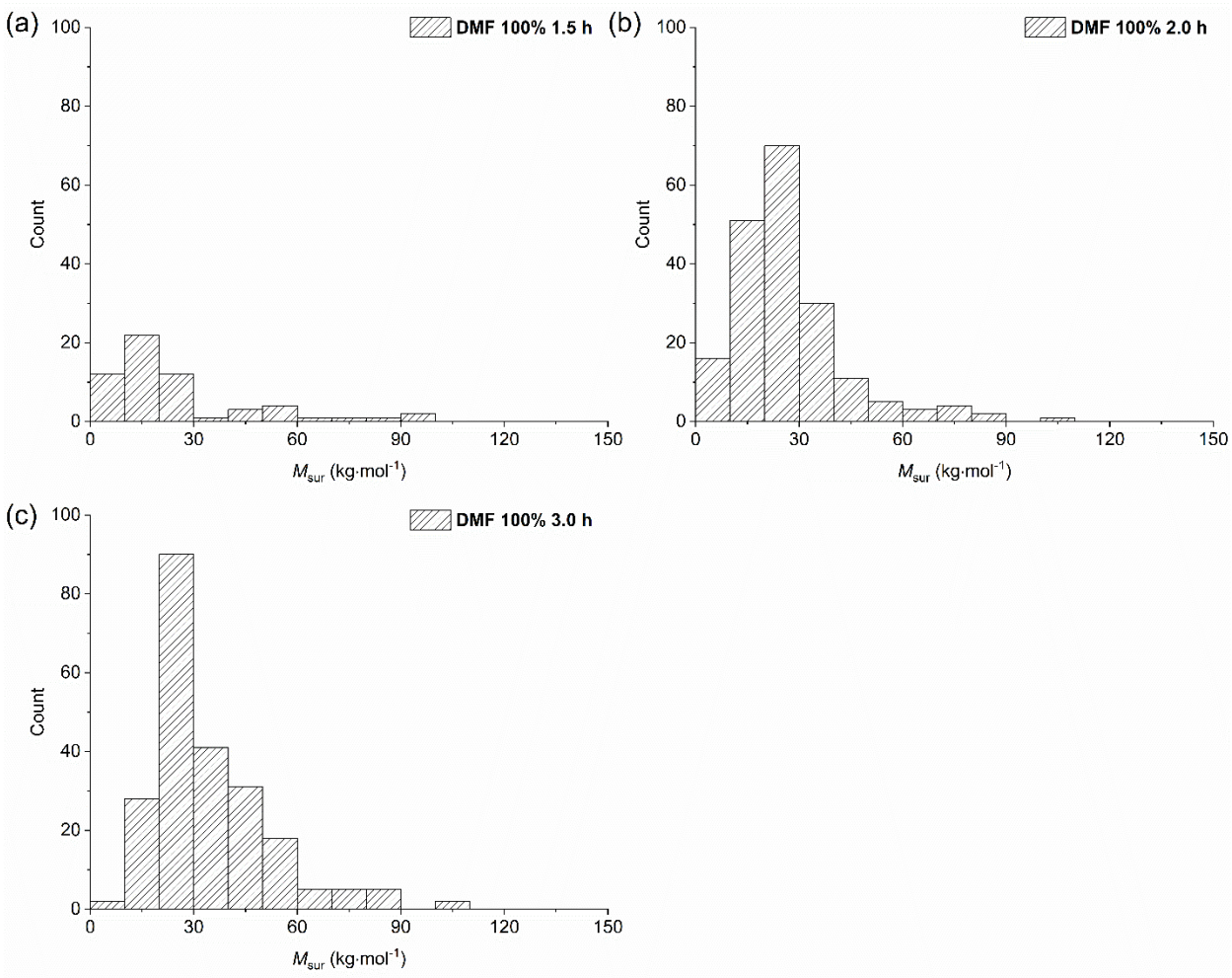

Figure S4. Molar mass M_{sur} distribution of surface-grafted polymer at (a) 1.5 h, (b) 2.0 h, and (c) 3.0 h at DMF 100% condition measured by SMFS.

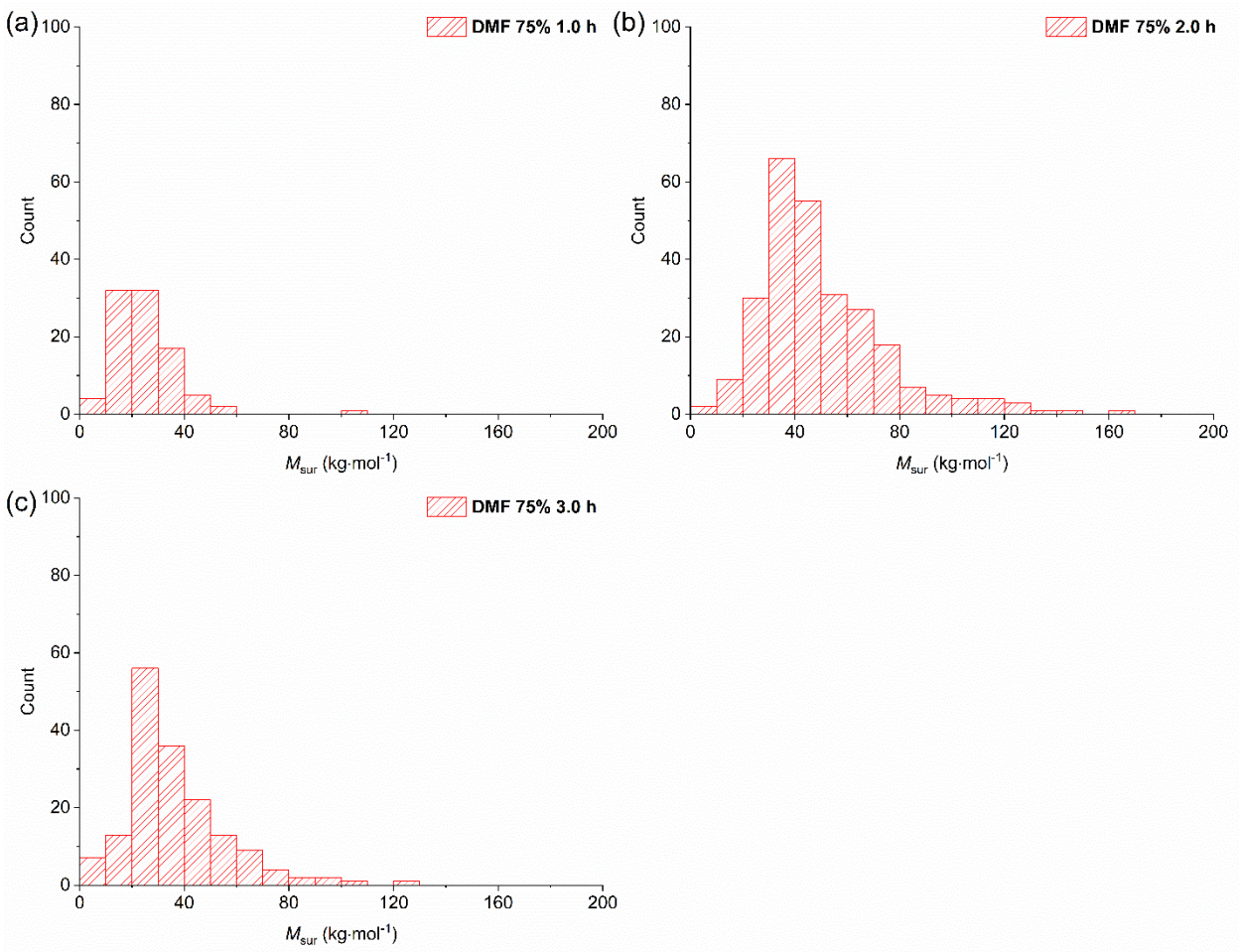

Figure S5. Molar mass M_{sur} distribution of surface-grafted polymer at (a) 1.0 h, (b) 2.0 h, and (c) 3.0 h at DMF 75% condition measured by SMFS.

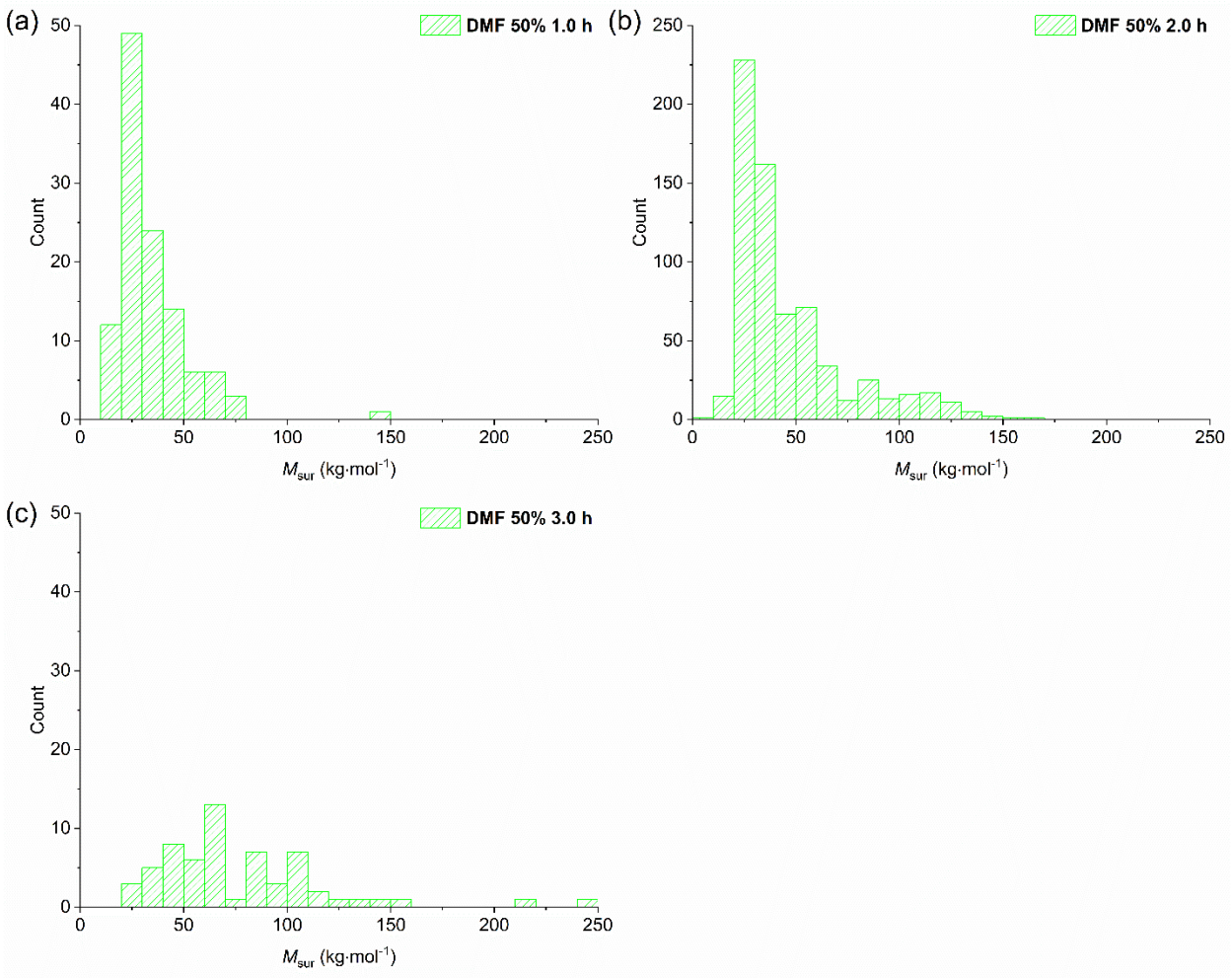

Figure S6. Molar mass M_{sur} distribution of surface-grafted polymer at (a) 1.0 h, (b) 2.0 h, and (c) 3.0 h at DMF 50% condition measured by SMFS.

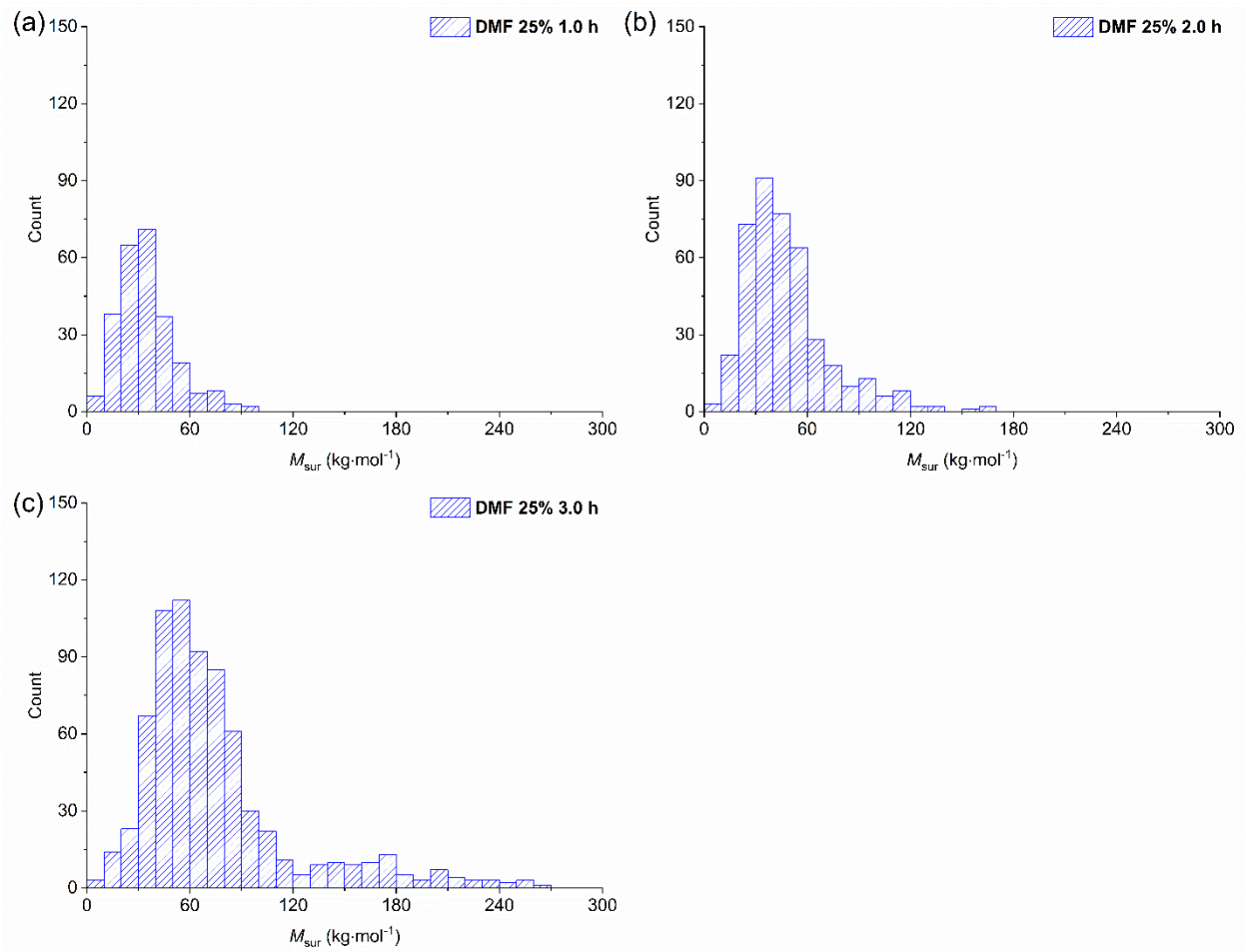

Figure S7. Molar mass M_{sur} distribution of surface-grafted polymer at (a) 1.0 h, (b) 2.0 h, and (c) 3.0 h at DMF 25% condition measured by SMFS.

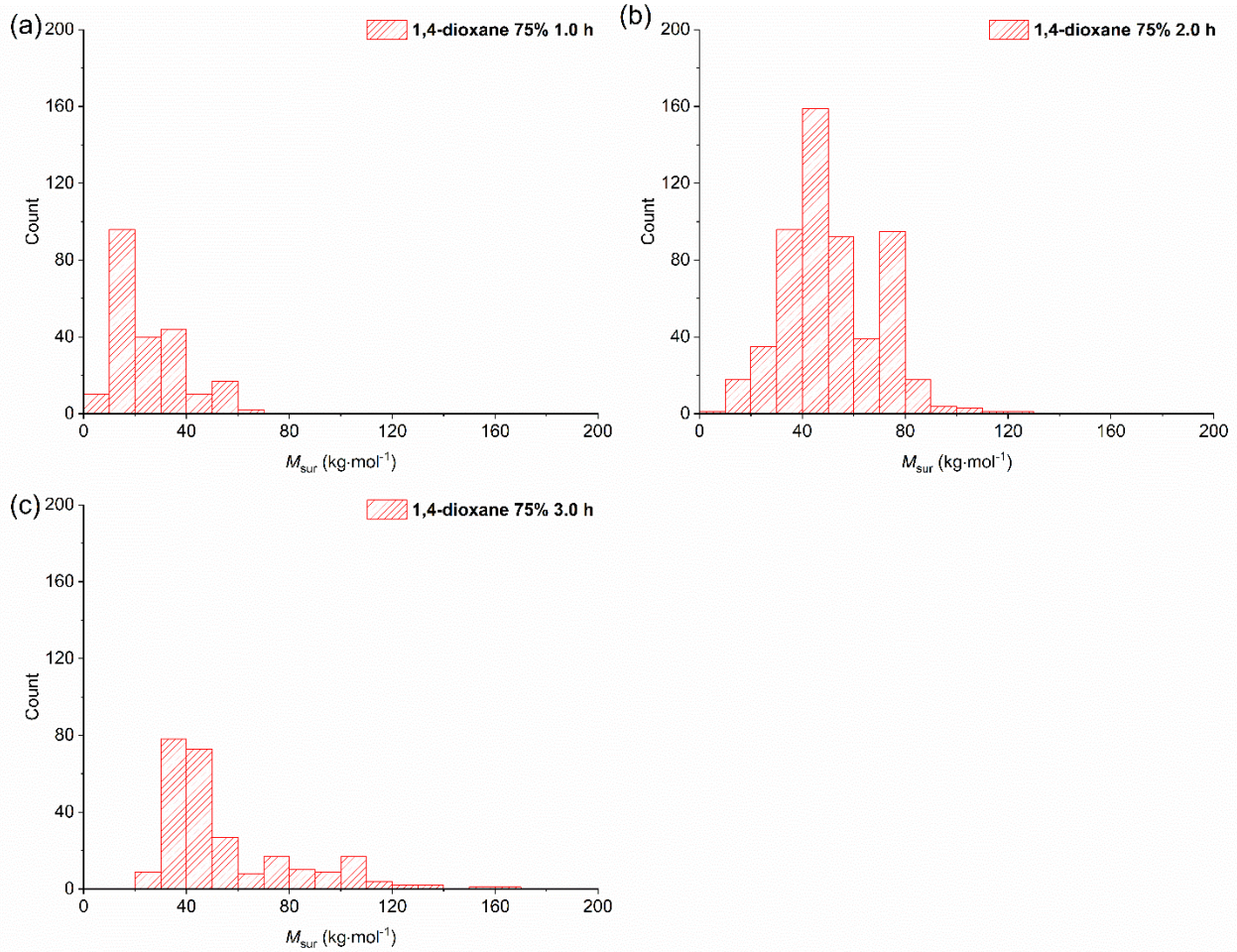

Figure S8. Molar mass M_{sur} distribution of surface-grafted polymer at (a) 1.0 h, (b) 2.0 h, and (c) 3.0 h at 1,4-Dioxane 75% condition measured by SMFS.

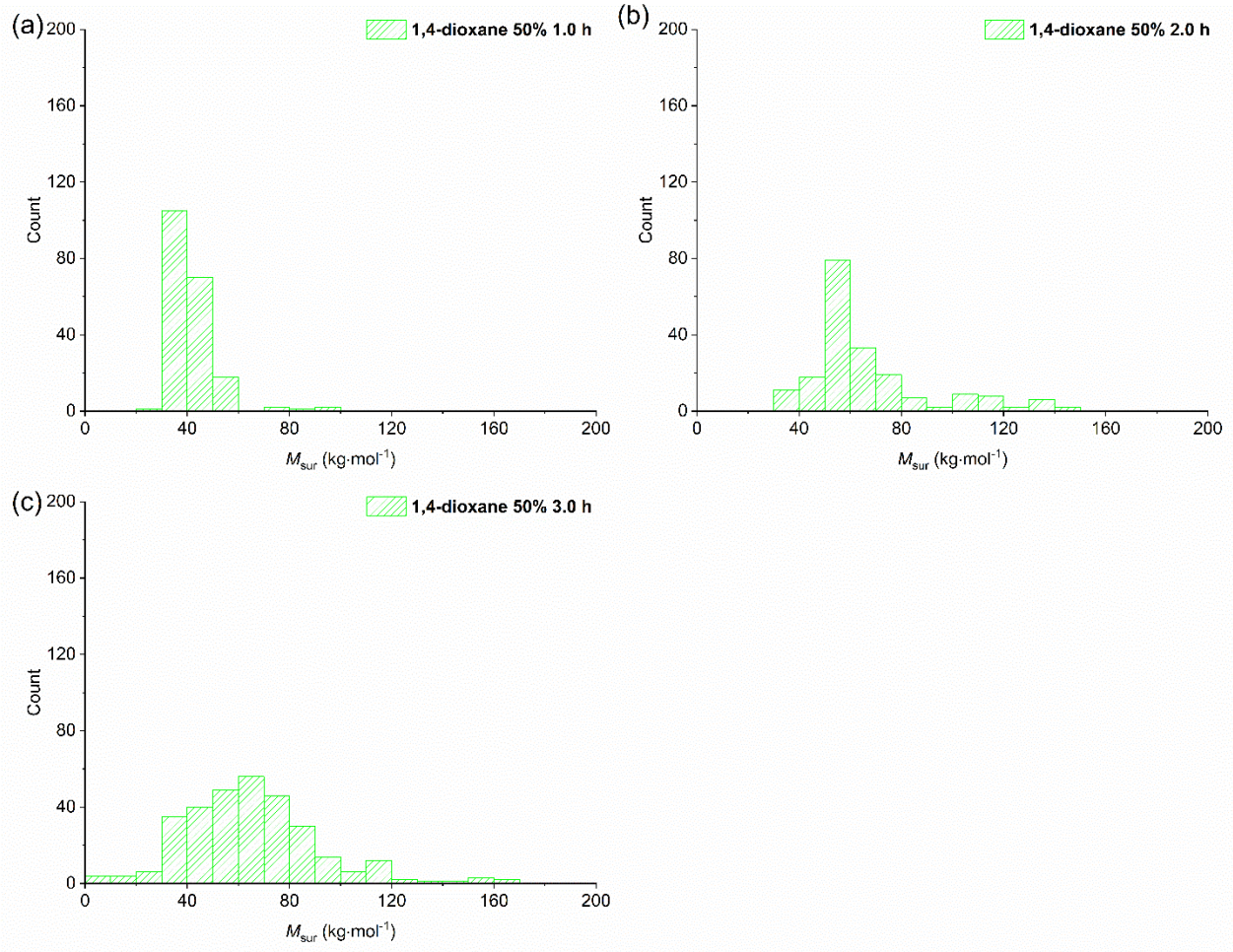

Figure S9. Molar mass M_{sur} distribution of surface-grafted polymer at (a) 1.0 h, (b) 2.0 h, and (c) 3.0 h at 1,4-Dioxane 50% condition measured by SMFS.

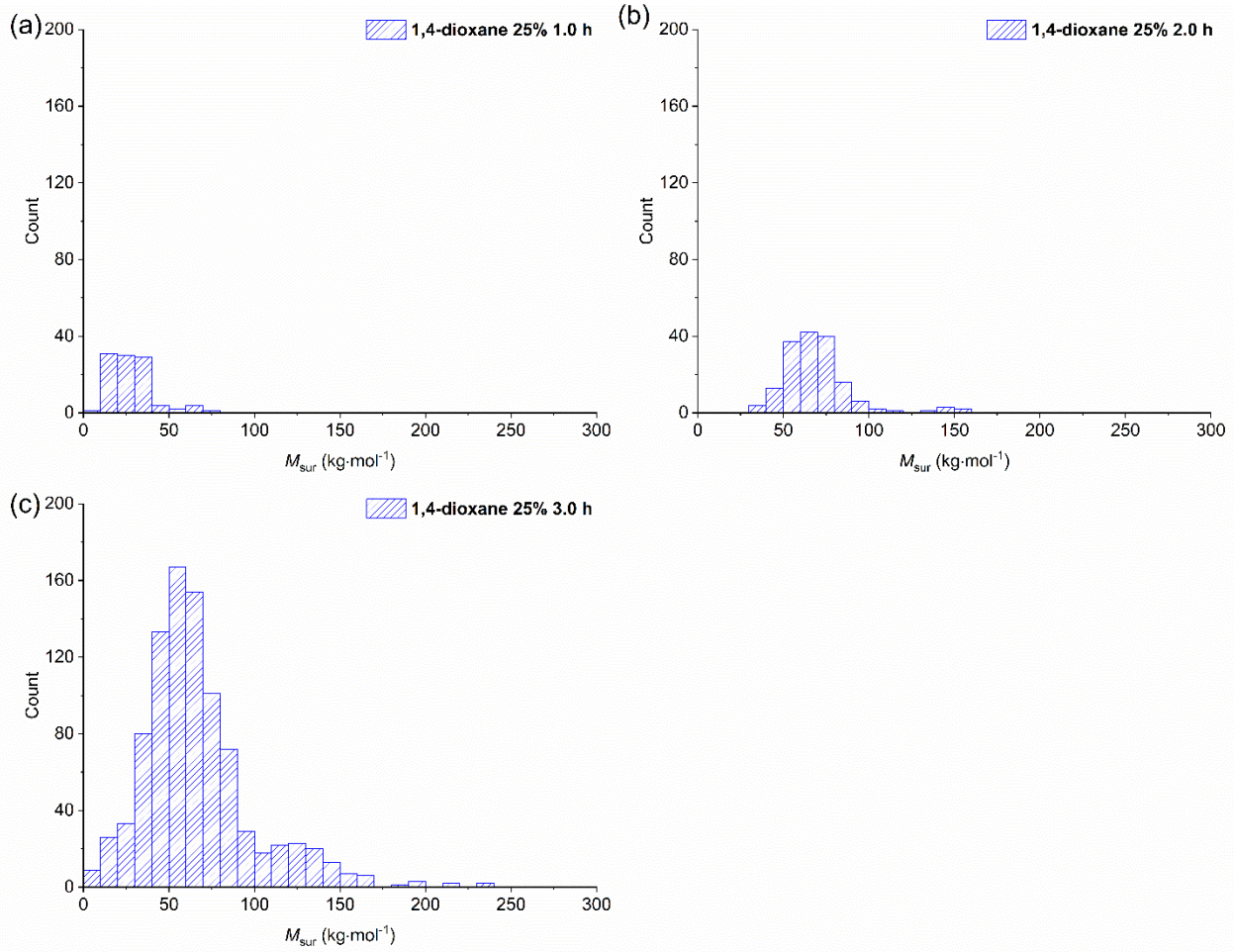

Figure S10. Molar mass M_{sur} distribution of surface-grafted polymer at (a) 1.0 h, (b) 2.0 h, and (c) 3.0 h at 1,4-Dioxane 25% condition measured by SMFS.

Calculation of the grafting density

The grafting density was calculated by the mass balance equation:

$$\sigma = \frac{h\rho N_A}{M_n} \qquad \text{(Equation S5)}$$

where the layer thickness (*h)* in the dry state was determined by SE, the bulk density (ρ) of p(HPMA) was taken to be 1.1 g·cm^{-3}, and N_A is the Avogadro constant. To obtain the grafting density from the thickness *h* and the number-average molar mass $M_{n,\,sur}$ (obtained by SMFS), the mass balance equation can be rewritten as:

$$M_n = \frac{1}{\sigma}(\rho N_A)h \qquad \text{(Equation S6)}$$

In Figure S11, $M_{n,\,sur}$ was plotted as a function of *h*. The grafting density σ was obtained from the linear regression fit of the dependence $M_{n,\,sur}$ *vs h* according to equation S6 (imposing a null *y*-axis intercept).[6-8]

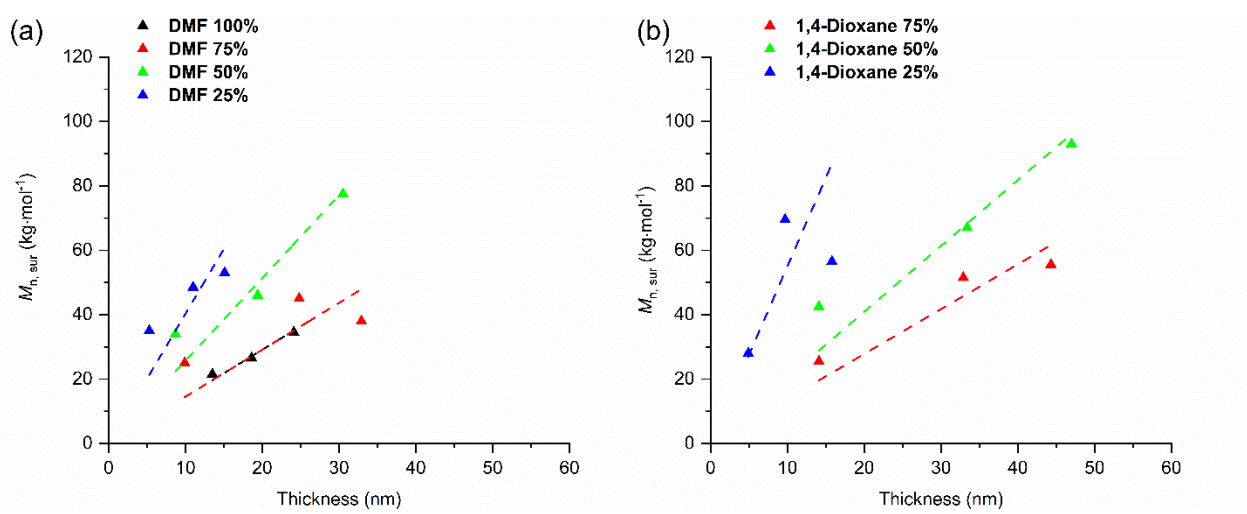

Figure S11. Surface-grafted p(HPMA) via SI-RAFT polymerization under various (a) DMF/water conditions and (b) 1,4-Dioxane/water conditions: $M_{n,\,sur}$ as a function of dry thickness, the dash lines represent the linear regression fits intercepting zero.

Table S3. Physical parameters of surface-grafted p(HPMA) in DMF condition.

Entry	Solvent conditions	Time (h)	Number-average $l_{n,c}$ (nm)	Number-average $M_{n,sur}$ (kg·mol^{-1})	h_{dry} (nm)	σ (chains·nm^{-2})
1	DMF 100%	1.5*	40.8	21.4	12.8	0.45
		2	50.3	26.4	16.3	
		3	65.9	34.6	24.2	
2	DMF 75%	1	47.8	25.1	10.4	0.45
		2	85.8	45.0	24.5	
		3	72.6	38.1	32.2	
3	DMF 50%	1	65.3	34.2	10.2	0.26
		2	88.1	46.2	21.4	
		3	147.3	77.3	25.6	
4	DMF 25%	1	66.6	34.9	5.4	0.16
		2	92.0	48.3	11.0	
		3	101.3	53.1	14.8	

Note: Each of the represented values is an average of at least two independent sets of measurements.
* The first selected reaction time of DMF 100% was 1.5 hour instead of 1.0 hour because the rupture curve overlapped with the adhesion jump of the force curve due to the relatively short chains.

Table S4. Physical parameters of surface-grafted p(HPMA) in 1,4-Dioxane condition.

Entry	Solvent conditions	Time (h)	Number-average $l_{n,c}$ (nm)	Number-average $M_{n,sur}$ (kg·mol^{-1})	h_{dry} (nm)	σ (chains·nm^{-2})
5	1,4-Dioxane 75%	1	48.4	25.4	15.0	0.48
		2	97.8	51.3	33.5	
		3	106.1	55.6	44.3	
6	1,4-Dioxane 50%	1	80.1	42.4	15.2	0.32
		2	128.1	67.2	34.2	
		3	177.7	93.2	45.7	
7	1,4-Dioxane 25%	1	53.0	27.8	4.9	0.14
		2	132.8	69.6	9.9	
		3	107.3	56.3	16.5	

Note: Each of the represented values is an average of at least two independent sets of measurements.

SI-RAFT polymerization of HPMA without free CTA in solution

A control experiment was performed to assess the impact of the added free CTA in the polymerization solution. For this, the polymerization was conducted identically as in the DMF 100% condition except that the addition of free CTA in the polymerization mixture was omitted. (Note: the Si substrates in the reactors will still be coated with a self-assembled monolayer functionalized with CTA). The results are presented in Figure S12 and compared with the DMF 100% condition, which included free CTA.

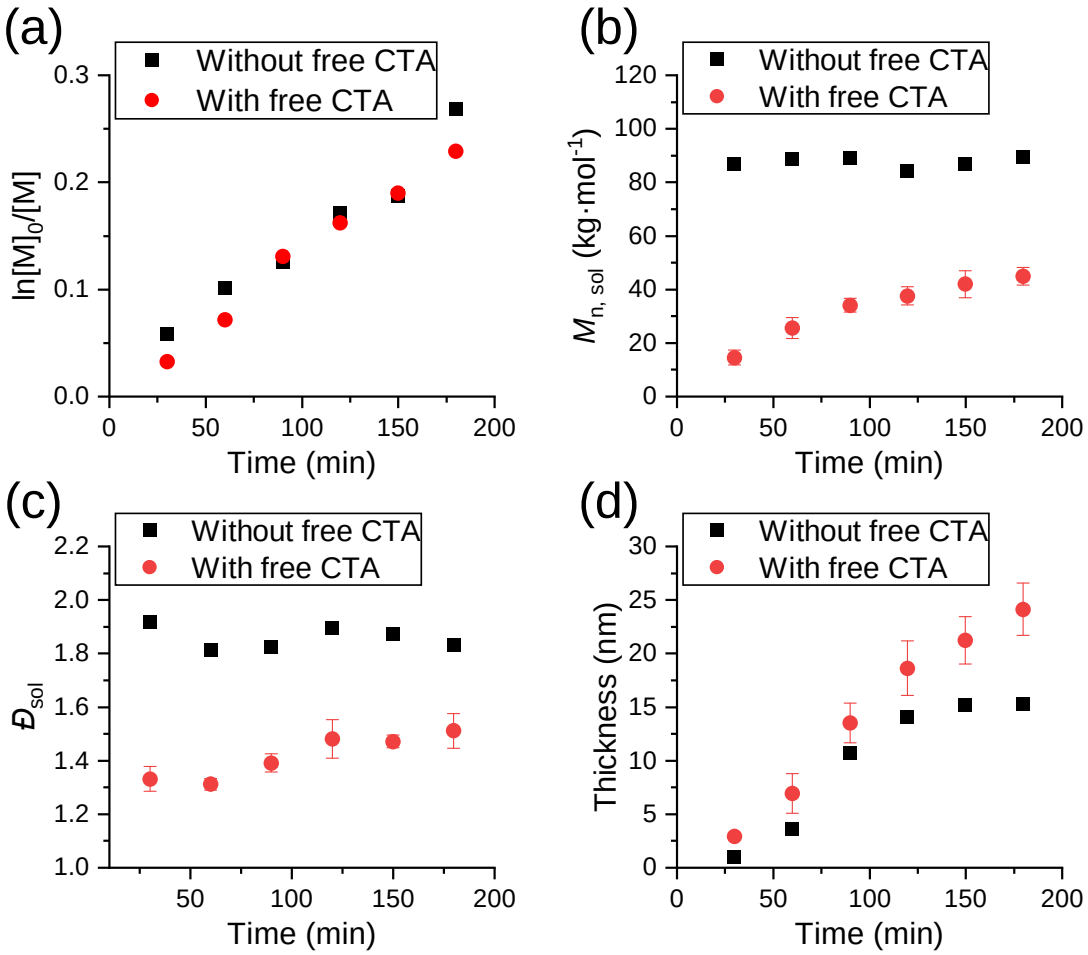

Figure S12. Comparison of polymerization kinetics of HPMA via SI-RAFT polymerization in DMF 100% with and with inclusion of free CTA in the polymerization solution: (a) conversion, (b) $M_{n,\,sol}$, (c) dispersity, and (d) thickness of the concurrently grown p(HPMA) layer against time. Individual values are reported in Table S5, ESI.

In solution, non-controlled free radical polymerization takes place (see chromatograms in Figure S13). The growth of the polymer from the surface slows down and stops after 2.0 h, indicating termination reactions probably due to loss of CTA. Following aminolysis of the samples. We attempted to carry out SMFS measurements to assess the molar mass distribution of the surface-grafted polymer. The resulting force-distance curves did not display clear unfolding–rupture events which could be assigned to Au-S binding between the polymer end-group and AFM tip (a representative force distance curve is shown in Figure S14). Non-specific interactions at relatively long tip–surface separation during retraction point to the presence of very long chains, suggesting uncontrolled growth of the polymer before loss of the CTA end group.

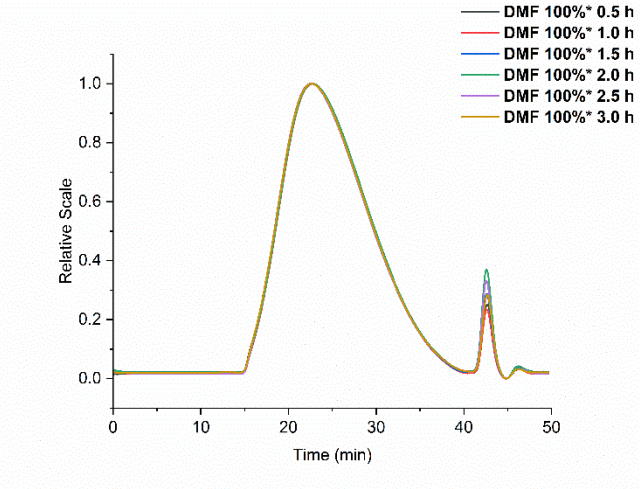

Figure S13. Evolution of SEC traces (differential refractive index detector) of solution-born p(HPMA) with different reaction times in the control experiment without addition of free CTA in DMF 100% condition (labeled as DMF 100%* in the figure).

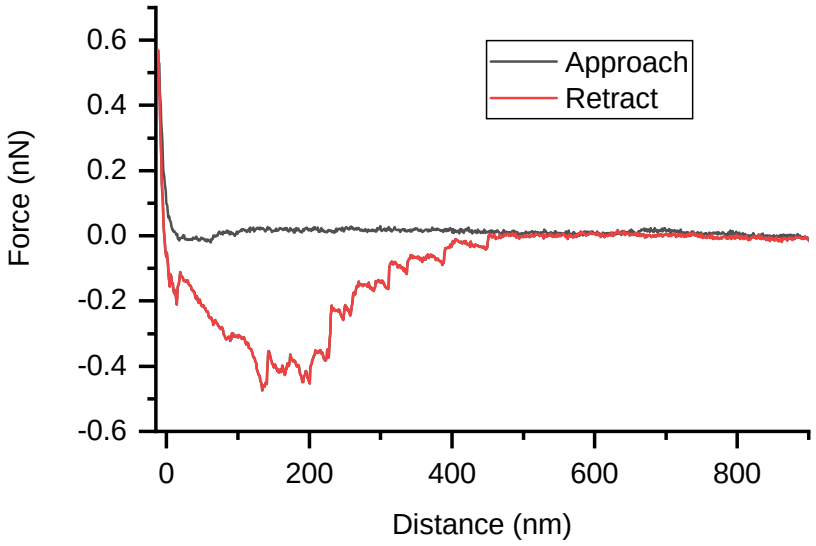

Figure S14. Representative force–distance curve obtained during SMFS measurement of the aminolyzed p(HPMA) layer obtained in the DMF 100% condition without addition of free CTA.

Table S5. Physical and macromolecular parameters of surface-grafted and solution-born p(HPMA) in DMF 100%* condition without free CTA.

Entry	Solvent conditions	Macromolecular parameters	Time (h)					
			0.5	1.0	1.5	2.0	2.5	3.0
1*	DMF 100%* without free CTA	Conversion (%)	5.7	9.6	11.8	15.7	17.1	23.5
		Number-average $M_{n,\,sol}$ ($kg \cdot mol^{-1}$)	86.6	88.8	89.1	84.4	86.7	89.3
		Dispersity, $Đ$	1.92	1.81	1.82	1.89	1.87	1.83
		h_{dry} (nm)	1.0	3.6	10.7	14.0	15.2	15.3

Scheme S1. Chemical structure of the surface-grafted p(HPMA) and illustration of inter- and intramolecular hydrogen bonding. (a) The inter-molecular hydrogen bonding between the water molecules and the side chains of the p(HPMA). (b) The hydrogen bonding between the side chains of the p(HPMA) in aprotic solvent.

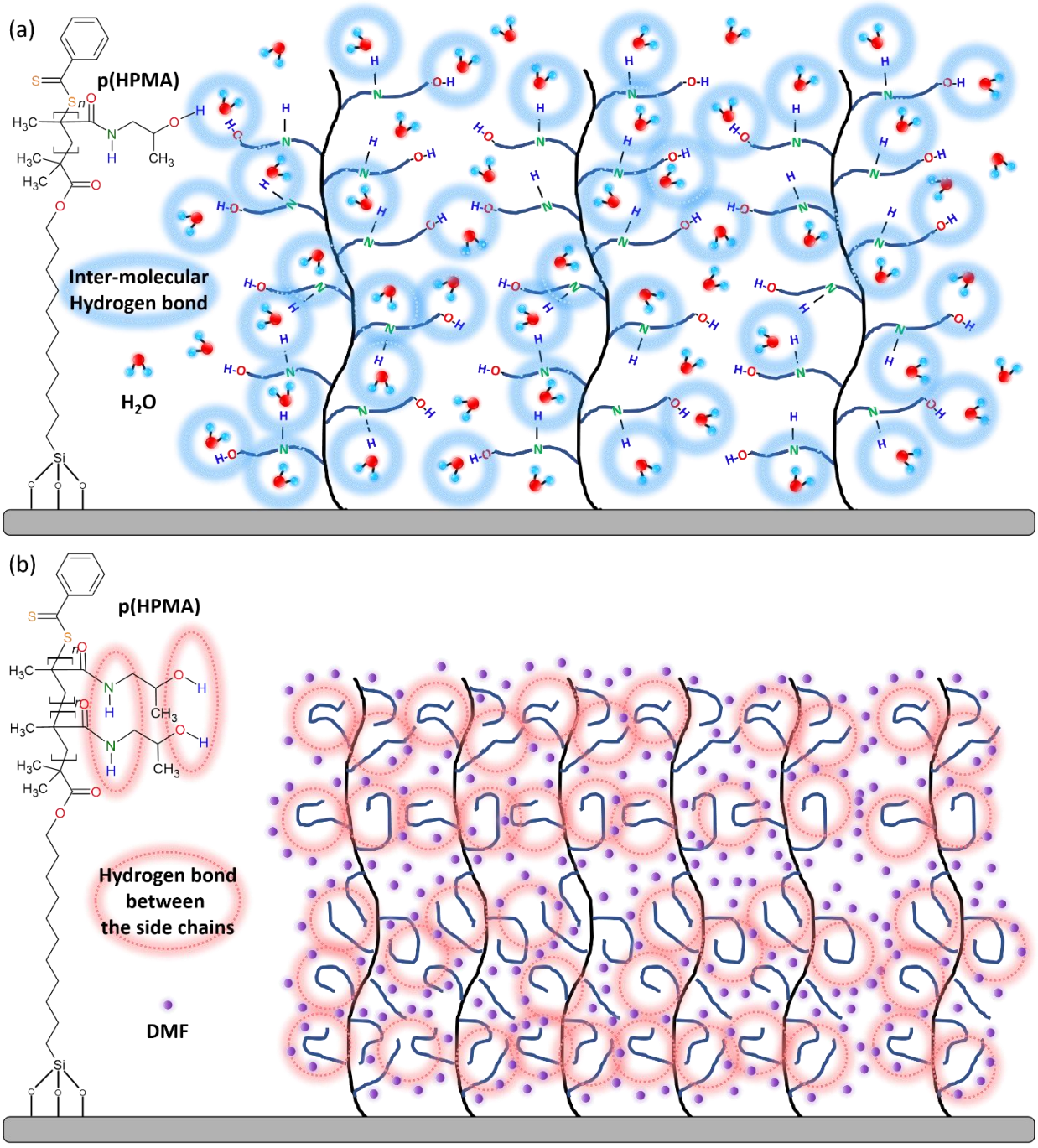

References

1. T. Tischer, R. Gralla-Koser, V. Trouillet, L. Barner, C. Barner-Kowollik and C. Lee-Thedieck, *ACS Macro Lett.*, 2016, **5**, 498-503.
2. A. R. Kuzmyn, M. van Galen, B. van Lagen and H. Zuilhof, *Polym. Chem.*, 2023, **14**, 3357-3363.
3. Y. Wang, A. Kálosi, Y. Halahovets, I. Romanenko, J. Slabý, J. Homola, J. Svoboda, A. de los Santos Pereira and O. Pop-Georgievski, *Polym. Chem.*, 2022, **13**, 3815-3826.
4. C. Bouchiat, M. D. Wang, J. Allemand, T. Strick, S. M. Block and V. Croquette, *Biophys. J.*, 1999, **76**, 409-413.
5. G. Meleshko, J. Kulhavy, A. Paul, D. J. Willock and J. A. Platts, *RSC Adv.*, 2014, **4**, 7003-7012.
6. R. R. Patil, S. Turgman-Cohen, J. Šrogl, D. Kiserow and J. Genzer, *Langmuir*, 2015, **31**, 2372-2381.
7. W. J. Brittain and J. Minko, *J. Polym. Sci., Part A.: Pol. Chem.*, 2007, **45**, 3505-3512.
8. J. L. Dalsin, L. Lin, S. Tosatti, J. Vörös, M. Textor and P. B. Messersmith, *Langmuir*, 2005, **21**, 640-646.